

Green Energy for Autonomous Devices: Surfactant-Enhanced Membraneless Hydrogen Peroxide Fuel Cells*

Fenyang Zhu,¹ Aleksei Kuzin,^{1,2} Guoxiang Chen,¹ Dmitry A. Gorin,² Brij Mohan,³ Gaoshan Huang,^{1,5,}
* Shuangliang Zhao,⁴ Yongfeng Mei^{1,5,6,7*} and Alexander A. Solovev^{1*}

Abstract— The amphipathic properties of surfactant macromolecules, characterized by their hydrophilic and hydrophobic terminal groups, are ubiquitously used to modulate the surface tension of interfaces and clean surfaces. Previously, the crucial role of surfactants was reported for the performance of catalytic nano- and micromotors. In this study, we extrapolate this concept to the membraneless hydrogen peroxide (H₂O₂) Fuel Cells (FCs), which exhibit performance dependence on the addition of different types of surfactants: cationic - Sodium Dodecyl Sulfate (SDS), anionic - Benzalkonium Chloride (BACl), and nonionic - Tween20. Among them, charged SDS and BACl show promotion and inhibition towards fuel cell performance, respectively. Non-charged Tween20 shows a neutral effect on fuel cell performance.

I. INTRODUCTION

The increased urgency for adopting clean energy sources is underscored by ongoing efforts to mitigate the usage of fossil fuels, reduce the global carbon footprint, tackle the problem of global warming, bridge the widening energy gap, and curtail severe air pollution. Hydrogen peroxide (H₂O₂), boasting an impressive energy density of 3.0 MJ l⁻¹ or 2.1 MJ kg⁻¹ for a 60% aqueous solution, stands as a competitive alternative to hydrogen (2.8 MJ l⁻¹, 3.5 MJ kg⁻¹ at 35 MPa) [1]. The membraneless, single-compartment configuration of H₂O₂ Fuel Cells (FCs) presents a simpler, cost-efficient advantage, bypassing the need for an electrolytic membrane (e.g., Nafion). Recent designs featuring three-dimensional electrodes in H₂O₂ FCs have accomplished a maximum areal power density of up to 300 W m⁻² [2]. Despite these advancements, the development of H₂O₂ FCs has encountered a bottleneck – the challenge of achieving technologically significant power outputs. This bottleneck can be attributed to the practical open circle potential (OCP) of membraneless H₂O₂ FCs being less than the theoretical value (1.09 V), stemming from simultaneous reduction and oxidation reactions of H₂O₂ on the cathode, leading to a mixed potential. Potential solutions may lie in developing a more selective electrocatalytic anode and cathode for H₂O₂ electrooxidation and electroreduction respectively, facilitating fuel-oxidant separation using laminar co-flows, ensuring prompt delivery and removal of

fuel/oxidant and reaction products, implementing redox couples, and applying high-surface area electrodes. A significant impediment in the progress of this approach is attributed to the energy-intensive requirement of fuel/oxidant pumping through high-surface-area electrodes, which is exacerbated by the elevated viscosity of laminar fluids. Addressing this issue, Mallouk and Sen introduced an innovative solution utilizing bimetallic catalytic nano- motors and pumps, harnessing the decomposition of H₂O₂ [3]. The mechanism involves the combination of protons and electrons with H₂O₂, resulting in the production of two H₂O molecules at the Au surface. Concurrently, the Pt surface undergoes H₂O₂ oxidation, leading to proton generation and subsequent transformation into O₂. The Pt and Au surfaces function as the cathode and anode, respectively, with the former facilitating H₂O₂ reduction and proton consumption and contributing to proton generation. These protons are then shuttled to the Pt surface (cathode) for utilization. Solovev and colleagues presented an efficient, miniaturized micro- motors and pump powered by the recoil of oxygen microbubbles [4]. The design employs optimal physicochemical properties such as reaction-diffusion phenomena, surfactants, and a specifically architected catalytic micropump, thus contributing to the advancement of this scientific domain. Progressing this concept further, the Hess group demonstrated the integration of self-powered catalytic pumps into a porous, membraneless H₂O₂ FC [5]. However, the research indicated that bubble nucleation on the electrode, particularly within ceramic membrane pores, at elevated concentrations of H₂O₂ adversely affected the FC's performance. Whitesides' group [6] demonstrated the concept of a membraneless laminar flow-based fuel cell (LFFC) operating at low Reynold numbers. In their design, fuel and oxidant are separated by the interface of laminar flow, eliminating the use of a proton exchange membrane (PEM), simplifying the fuel cell architecture. However, the delivery of laminar fuels/oxidants requires high pumping pressure, leading to increased energy cost.

Hydrogen peroxide (H₂O₂) has recently emerged as a focus of intense scientific interest due to its unique, environmentally friendly attributes.[7-9] The decomposition of H₂O₂ yields

[†]This work was supported by the National Key Technologies R&D Program of China (2021YFA0715302 and 2021YFE0191800), the National Natural Science Foundation of China (61975035 and 52150610489), and the Science and Technology Commission of Shanghai Municipality (22ZR1405000).

¹Department of Materials Science & State Key Laboratory of Molecular Engineering of Polymers, Fudan University, Shanghai 200433, P. R. China. E-mail: solovevlab@gmail.com

²Center for Photonic Science and Engineering, Skolkovo Institute of Science and Technology, 121205 Moscow, Russia

³Centro de Quimica Estrutural, Institute of Molecular Sciences, Instituto Superior Tecnico, Universidade de Lisboa, Av. Rovisco Pais, 1049-001 Lisboa, Portugal

⁴Guangxi Key Laboratory of Petrochemical Resources Processing and Process Intensification Technology and School of Chemistry and Chemical Engineering, Guangxi University, Nanning, 530004, P. R. China

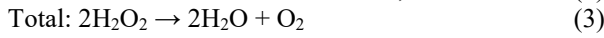
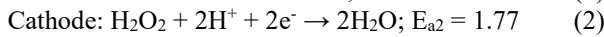
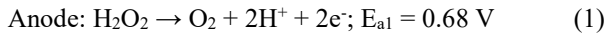
⁵International Institute of Intelligent Nanorobots and Nanosystems, Fudan University, Shanghai 200433, P. R. China

⁶Shanghai Frontiers Science Research Base of Intelligent Optoelectronics and Perception, Fudan University, Shanghai 200433, P. R. China

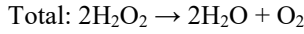
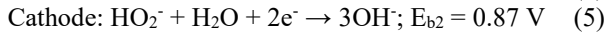
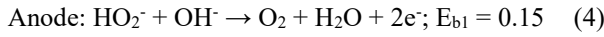
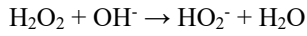
⁷Yiwu Research Institute of Fudan University, Yiwu 322000, Zhejiang, P. R. China

water (H₂O) and oxygen (O₂), aligning with sustainability goals. Furthermore, its remarkable disproportionation reaction [10] enables H₂O₂ to act as fuel and oxidant, obviating the need for a Proton Exchange Membrane (PEM) and laminar flow conditions. In a seminal work, Yamasaki *et al.* [8] elucidated the function of their Membraneless H₂O₂ Fuel Cells (MHPFCs) demonstrated that the electrooxidation and electroreduction reactions selectively localized at the cathode and anode, respectively. Since then, numerous subsequent studies [11-14] have been conducted to enhance the performance of MHPFCs. The specific reactions governing the operation of these FCs can be represented as follows (E vs. SHE) [15, 16]:

Reactions in the acidic media:



Reactions in the basic media:



It is known that the theoretical open circuit potential (OCP) of MHPFC is 1.09 V (in acidic media) and 0.62 V (in basic media) [15, 16]. However, experimental results show far below OCPs due to the limited selectivity of electrodes and self-decomposition of H₂O₂ on electrodes [15,17]. And power output of MHPFC is not enough to satisfy practical applications.

In this study, we explored the influence of surfactants in modulating the performance of the MHPFC. The Ni foam and Au electroplated carbon fiber cloth showed excellent selectivity and catalytic performance towards the ERR and EOR, respectively. A comprehensive analysis has been performed using anionic (SDS), cationic (BACl), and nonionic (Tween20) surfactants.

II. MATERIALS AND METHODS

This section introduces the primary materials, reagents, and methods for installing the MHPFC system. In subsection A, all materials and reagents are listed in detail. Procedures for obtaining electrodes of MHPFC are included in subsection B. In subsection C, the structural characterization of electrodes is illustrated. In the last subsection, MHPFC performance characterization is shown.

A. Materials and Reagents

Commercially available Nickel-foam and carbon fiber cloth, with dimensions of 25mm x 25mm, were utilized. A Gold Chloride Trihydrate (HAuCl₄) solution facilitated the electroplating of gold onto carbon fiber cloth, creating a high surface area electrode. The electrolyte comprised H₂O₂, surfactants (SDS, BACl, and Tween20), and pH regulators (NaOH, HCl). Experimental parameters involved setting H₂O₂ concentration at 1M and varying surfactants' concentrations at 0 mM, 0.1 mM, 1 mM, 10 mM, and 100 mM.

B. Electrodes Fabrication Procedure

A facile electroplating method was adopted to fabricate a three-dimensional, high-surface area cathode. The carbon fiber cloth was pre-processed by sequentially rinsed with acetone, alcohol, and deionized water thrice. The Electrochemical Station (ECS, Shanghai Chenhua Instrument Co., Ltd., CHI600E) was used as an electroplating device with three electrodes method: carbon fiber cloth as the Working Electrode (WE), graphite rod as the Counter Electrode (CE), and Ag/AgCl (saturated 1 M KCl solution) as the Reference Electrode (RE). The electroplating parameters were established using Multi-Potential Steps: E_{work} : 0.3 V, 0.2 s; E_{rest} : 0.1 V, 0.1 s. The rest period was set for the uniform diffusion of Au³⁺ in diluted HAuCl₄ solutions. A circle consisted of one work and rest period with 1600 circles (*Fig. 1*).

C. Structural Characterization of Electrodes

To characterize the performance of Au electroplated carbon fiber cloth, X-Ray Diffraction (XRD, Bruker Corporation, D8 Advance) and Scanning Electron Microscopy (SEM, Carl Zeiss AG, EVO 10) were used. XRD was taken to confirm Au on carbon fiber cloth. SEM was conducted to characterize distributions of Au nanoparticles (NP).

D. Performance Characterization of MHPFCs

Performance characterizations were conducted using an electrochemical station. TMHPFC performance was evaluated under varying solution conditions established across multiple experimental groups. The first group explored the effects of proton/hydroxyl ion H⁺/OH⁻ concentration (pH=1, 3, 5, 7, 9, 11, 13) on MHPFC performance. The second group was designed to analyze the type of surfactant (cationic, anionic, and nonionic) on MHPFC performance. The final group aimed to elucidate the influence of specific surfactant concentrations on MHPFC performance.

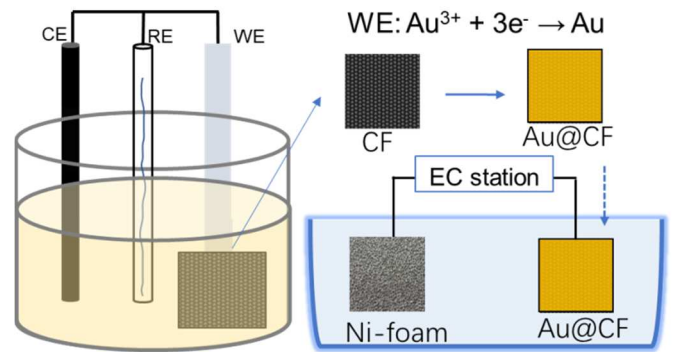


Figure 1. Electroplating method for fabricating Au@CF cathode of MHPFCs. Electroplating electrolyte consists of 5 mM HAuCl₄, 0.1M HCl and 0.1 M KCl.

III. RESULTS

Fig. 2 shows the structural characterization results of XRD and SEM images. In *Fig. 2(a)*, XRD results indicate clear peaks at 38.19°, 44.39°, 64.58° and 77.60° corresponding to the (111), (200), (220), and (311) crystal planes of face-centered cubic (fcc) Au. SEM images shown in *Fig. 2(b-c)* have seen detectable Au nanoparticles grown and distributed on the carbon fiber cloth. All results have proved successfully electroplated onto the carbon fiber cloth.

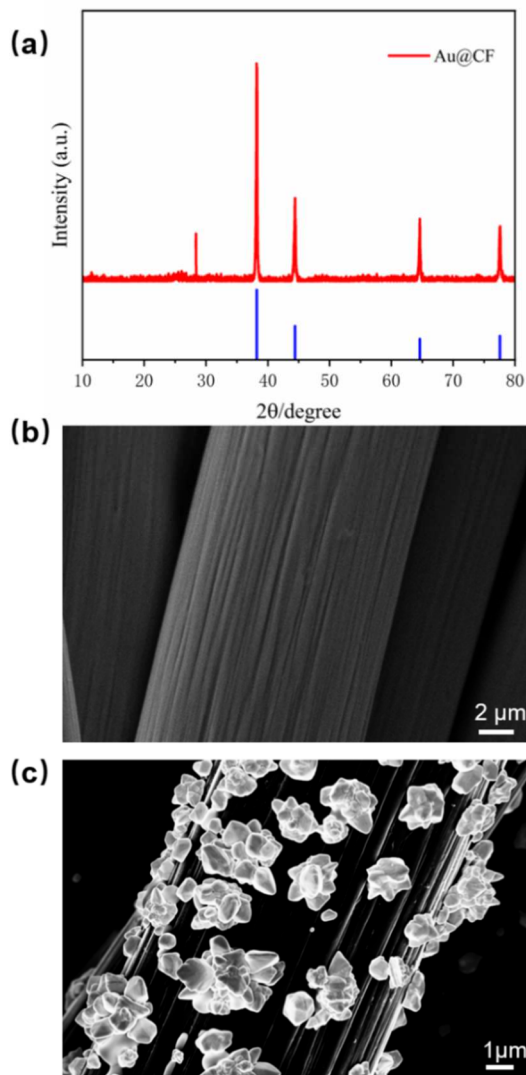


Figure 2. structural characterization of Au@CF. (a) XRD result of Au@CF, (b) SEM images of CF after pre-process, (c) SEM image of Au@CF distributed with Au nanoparticles.

Furthermore, the optimization of pH conditions is critical for the stability and efficacy of the H₂O₂ decomposition reaction. Based on reactions (1)(2) and (4)(5), it can be inferred that both H⁺/OH⁻ ions can act as catalysts to enhance the reaction rate of H₂O₂ electrochemical reactions. Experimental results, as shown in Fig. 3, validate the hypothesis that the MHPFC performance is superior in acidic (pH = 1) and basic (pH = 13) solutions compared to intermediate pH levels. The electrochemical activity at distinct pH levels, as revealed by cyclic voltammetry, underscores the distinct catalytic pathways these ions undertake. Under pH = 13 conditions, the Open Circuit Potential (OCP) and Maximum Current Density (MCD) are lower than under pH = 1 conditions. This observation is attributed to the intense self-decomposition process of H₂O₂, as observed in our experiments.

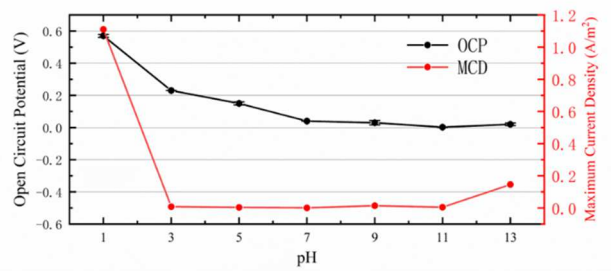


Figure 3. OCP and MCD of MHPFC under different pH in 1M H₂O₂ solutions

The results demonstrate a significant influence of surfactants presence in solution on MHPFCs performance seen in Fig. 4. The addition of SDS to the MHPFC electrolyte enhanced the performance, with the maximum power output being three times higher than in a non-SDS electrolyte, as shown in Fig. 4(a). Conversely, including BACl, even in minute quantities (0.1 mM), decreased MHPFC performance, particularly in power output, with a continuous decrease observed with adding more BACl, as shown in Fig. 4(b). The non-ionic surfactant Tween20, in Fig. 4(c), did not noticeably affect the MHPFC performance. Our preliminary hypotheses suggest that charged surfactants can accumulate at the interface between the electrolyte and electrode and modify interactions between H₂O₂ molecules and electrodes and facilitate the electron transfer in between.

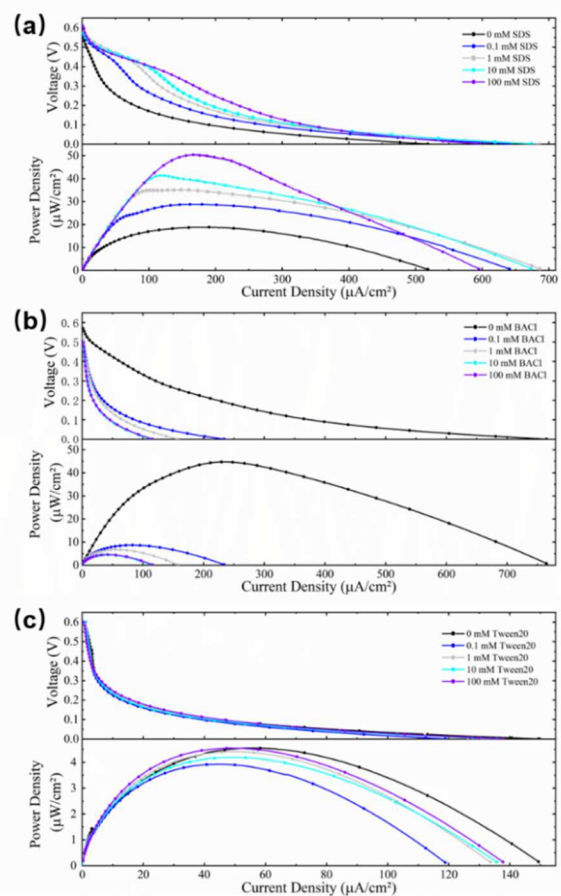


Figure 4. MHPFC performance. (a) OCP and MCD of MHPFC under different pH in 1M H₂O₂ solutions; polarization and power output curves of (A) SDS, (B) BACl, (C) Tween20 in 1 M H₂O₂, pH=1 solutions.

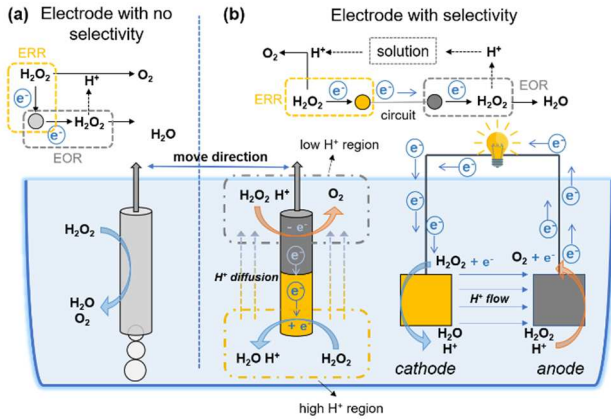


Figure 5. Micro-motors and fuel cell powered by hydrogen peroxide decomposition. (a) Schematic image of H_2O_2 -powered tubular micromotor. (b) left: schematic of H_2O_2 -powered motor driven by self-electrophoresis; right: schematic of H_2O_2 -powered MHPFCs.

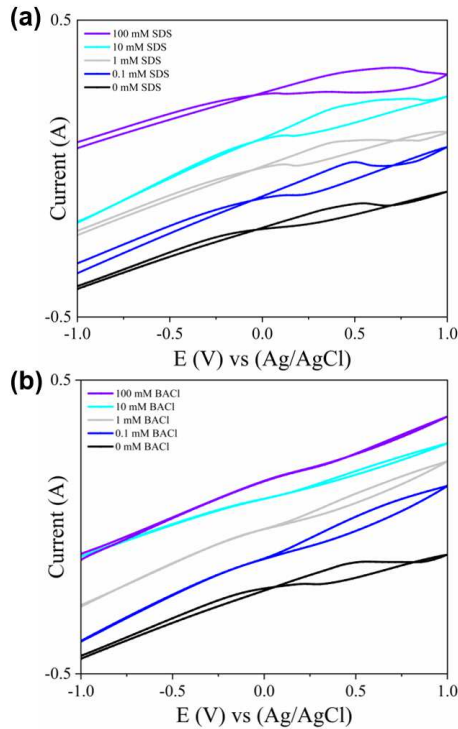


Figure 6. Cyclic voltammetry (CV) curve of Ni-foam using different concentrations of surfactants (SDS, BACl). The scan rate is 0.01 V/s.

IV. DISCUSSION

In 1 M aqueous solutions of H_2O_2 incorporating sodium dodecyl sulfate (SDS), a marginal increase in the open circuit potential (OCP) can be observed, from 0.55 V to 0.61 V (Fig. 4). Simultaneously, the maximum power output exhibited an increase to $50.6 \mu\text{W cm}^{-2}$ in the presence of 100 mM SDS, which is nearly three-fold higher compared to the condition where SDS was not present ($18.88 \mu\text{W cm}^{-2}$). This outcome implies the potential for SDS to modulate the performance of MHPFCs effectively. Regarding the anionic surfactant BACl, a pronounced decrease in MHPFC performance was observed. In the absence of BACl, the maximum power output was recorded to be $44.76 \mu\text{W cm}^{-2}$, whereas in the presence of only

0.1 mM BACl solutions, the power output decreased drastically to $8.69 \mu\text{W cm}^{-2}$. This reduction in power output suggests a significant alteration of the interface electrochemical process, attributable to the introduction of BACl. Contrarily, the non-ionic surfactant Tween20 did not demonstrate any discernible influence on the performance of the MHPFC. The OCP and maximum power output measurements were within the range of statistical error, with an average maximum power output of $4.43 \mu\text{W cm}^{-2}$ and a standard deviation of 0.42. Similarly, the OCP remained stable in the presence of Tween20, ranging between 0.52 V and 0.55 V, with an average OCP of 0.538 V and a standard deviation of 0.011. This observation suggests that Tween20 does not affect the performance of the MHPFC under the given experimental conditions.

Previously, a critical role of surfactants was reported for the operation of bubble-propelled catalytic micro-/nanomotors powered by the catalytic decomposition of H_2O_2 . [18-20] Subsequent studies [21, 22] demonstrated the influence of surfactants on bubbles evolution (nucleation, generation, diameter, recoil frequency) with initial attempts to lower the surface tension and alter the Zeta potential (ZP) of surfaces. The H_2O_2 electrooxidation reaction (EOR) and electroreduction reaction (ERR) can occur at the same active point of non-selective catalyst material, shown in Fig. 5(a). Fig. 5(b) illustrates the mechanism of using selective electrocatalysts, which separate EOR and ERR at two different materials, enabling the motion of micromotors [23] and MHPFCs [11]. One main difference between catalytic nano-/micromotors and fuel cells: anode and cathode are connected in NMs, while anode and cathode are separated in MHPFCs. Our experiments, use MHPFC commercially available Ni-foam as an anode and Au electroplated carbon fiber cloth (Au@CF) as a cathode. By controlling the amounts of surfactants added to the electrolyte, we explored how the concentration and types of surfactants influence MHPFCs performance. MHPFCs that utilized the cationic surfactant SDS demonstrated a threefold increase in maximum power output, compared to those under non-surfactant conditions, as shown in Fig. 4(a). Anionic BACl resulted in a sharp decrease in power output, and nonionic Tween20 had a neutral effect on MHPFC performance, as depicted in Fig. 4(b-c). Surfactants play a complex and multifaceted role in modulating the performance of MHPFCs.

Here we proposed a potential explanation of surfactants impact on fuel cells. According to research [24, 25], $\text{Ni}(\text{OH})_2$ groups at the surface of Ni anode play a vital role in the H_2O_2 oxidation reaction. Besides, cyclic voltammetry (CV) results [24] indicate that the oxidation and reduction window of the $\text{Ni}(\text{OH})_2$ group is around 0.2 V to 0.5 V (vs. Ag/AgCl). Fig. 6 shows CV results towards the Ni electrode. It is clearly observed that with the increasing concentration of SDS, the characteristic peak of $\text{Ni}(\text{OH})_2$ appears, as shown in Fig. 6(a). In contrast, with the increasing concentration of BACl, the characteristic peak of $\text{Ni}(\text{OH})_2$ disappears, as shown in Fig. 6(b). We assume that surfactants can protect/inhibit specific groups at the electrode surface, thus changing the overall electrochemical reaction process. However, surfactants may have other significant roles in the electrochemical process. In the context of MHPFCs, the anionic SDS appears to enhance FC's performance. SDS molecules can be adsorbed on the

surface of the electrode, altering its physicochemical properties such as wettability and distribution of charge. Subsequently, it can impact the electrode-electrolyte interface, potentially facilitating the electrochemical reactions with H_2O_2 , resulting in the power output change. Conversely, the cationic BACl surfactant negatively affects the MHPFC performance. BACl, being positively charged, can interfere with the electrostatic interactions at the electrode-electrolyte interface, possibly hindering the necessary reactions for power generation. Additionally, the surfactant can also induce an unfavorable modification of the electrode surface, potentially by adsorption, leading to a decrease in the power output. The non-ionic surfactant Tween20 does not appear to impact MHPFC performance significantly. Due to its neutral charge, Tween20 likely does not induce notable electrostatic changes at the electrode-electrolyte interface, nor does it alter the surface properties of the electrode. Thus, it is plausible that Tween20 presence does not markedly influence the electrochemical reactions involving H_2O_2 .

Overall, our preliminary hypotheses underscore the significance of surfactants in manipulating MHPFC performance, likely through altering interfacial interactions and modulating the physicochemical properties of the electrode. Further rigorous investigations are essential to establish the exact mechanisms of surfactant action in MHPFCs unequivocally. However, it should be emphasized that the precise effects of surfactants on MHPFCs are likely to be specific to the surfactant structure, the fuel cell architecture, and the nature of the electrodes and electrolytes. Furthermore, the impact of surfactants on MHPFC performance is likely not solely due to their direct interactions at the electrode-electrolyte interface, but also their overall effect on the physicochemical properties of the system, including potential changes in the solution's viscosity, conductivity, and related parameters. While this discussion provides a feasible explanation for the observed behaviors, these are, as noted, our preliminary hypotheses. Further research is required to validate the role of surfactants and to elucidate their underlying mechanism of action, such as surface characterization of electrodes, investigation of reaction kinetics, and computational modeling to provide a more holistic understanding of the phenomena.

V. CONCLUSION

As the field of nanomotors has progressively delineated itself, surfactants have been ubiquitously employed to modulate surface tension and enhance the stability of microbubbles. Intriguingly, observations suggested that the specific category of surfactant exerts a discernible influence on the kinematics of catalytic nanomotors. However, a comprehensive exploration of this phenomenon remained pending. In juxtaposition, the incorporation of surfactants in fuel cell research remains conspicuously absent. Our results accentuate the merits of a synergistic and interdisciplinary research approach. The advancements in H_2O_2 fuel cell (FC) technology present an innovative conceptual framework, wherein H_2O_2 is concurrently utilized as both fuel and oxidant within a monolithic device architecture. Our empirical investigation aimed to systematically evaluate the potential of

surfactants in the electrolyte for enhancing micro- H_2O_2 fuel cell (MHPFC) performance. Initial findings indicated that the anionic surfactant, sodium dodecyl sulfate (SDS), could indeed augment MHPFC performance. Nevertheless, the intricate mechanistic details underlying the function of surfactants in MHPFCs necessitate further intensive investigation. The acquired knowledge could then be broadly disseminated and applied across various FC technologies, employing surfactants as performance modulating agents. Theoretically, H_2O_2 FCs can achieve a maximal electrochemical potential of 1.09 V, establishing a competitive edge analogous to methanol/air FCs (1.21 V) and H_2 /air FCs (1.23 V). Moreover, H_2O_2 exhibits a remarkable compatibility with a diverse array of fuels, encompassing ethanol, formic acid, specific metals (e.g., magnesium), and hydrazine. Furthermore, the integration of H_2O_2 with alternative fuels/oxidants or the utilization of redox couples could conceivably result in power densities on the order of kW m^{-2} .

ACKNOWLEDGMENT

The authors would like to thank Prof. Valeri Tolstoy of St. Petersburg State University for his valuable discussions and insights.

REFERENCES

- [1] M. Hirscher, "Handbook of hydrogen storage", *Topics in Applied Physics*, vol. 12, 2010.
- [2] Y. Yang, H. Zhang, J. Wang, S. Yang, T. Liu, K. Tao, and H. Chang, "A silver wire aerogel promotes hydrogen peroxide reduction for fuel cells and electrochemical sensors," *Journal of Materials Chemistry A*, vol. 7, no. 18, pp. 11 497–11 505, 2019.
- [3] S. Das, O. E. Shklyae, A. Altemose, H. Shum, I. Ortiz-Rivera, L. Valdez, T. E. Mallouk, A. C. Balazs, and A. Sen, "Harnessing catalytic pumps for directional delivery of microparticles in microchambers," *Nature Communications*, vol. 8, no. 1, p. 14384, 2017.
- [4] A. A. Solovlev, S. Sanchez, Y. Mei, and O. G. Schmidt, "Tunable catalytic tubular micro-pumps operating at low concentrations of hydrogen peroxide," *Physical Chemistry Chemical Physics*, vol. 13, no. 21, pp. 10 131–10 135, 2011.
- [5] I.-K. Jun and H. Hess, "A biomimetic, self-pumping membrane," *Advanced Materials*, vol. 22, no. 43, pp. 4823–4825, 2010.
- [6] R. Ferrigno, A. D. Stroock, T. D. Clark, M. Mayer, and G. M. Whitesides, "Membraneless vanadium redox fuel cell using laminar flow," *Journal of the American Chemical Society*, vol. 124, no. 44, pp. 12 930–12 931, 2002.
- [7] Z.Y. Yang, Z.X. Wei, S.X. Zhou, B. Bao, S.L. Zhao, and F.Z. Gong, "Direct thermal catalytic synthesis of hydrogen peroxide by using microchip reactor," *The Chemical Engineering Journal*, vol. 456, no. 24, 140915, 2023.
- [8] J.J. Qiu, W.Q. Tang, B. Bao, and S.L. Zhao, "Microfluidic-based in-situ determination for reaction kinetics of hydrogen peroxide decomposition," *The Chemical Engineering Journal*, vol. 424, no. 15, 130486, 2021.
- [9] M.M. Yan, Z.X. Wei, Z.C. Gong, B. Johannessen, G.L. Ye, G.C. He, J.J. Liu, S.L. Zhao, A. Cui, and H.L. Fei, "Sb₂S₃-templated synthesis of sulfur-doped Sb-N-C with hierarchical architecture and high metal loading for H_2O_2 electrosynthesis," *Nature Communications*, vol. 14, no. 1, p. 368, 2023.
- [10] F. Jaouen and J.-P. Dodelet, "O₂ reduction mechanism on non-noble metal catalysts for pem fuel cells. part i: Experimental rates of o₂ electroreduction, H_2O_2 electroreduction, and H_2O_2 disproportionation," *The Journal of Physical Chemistry C*, vol. 113, no. 34, pp. 15 422–15 432, 2009.

- [11] S.-i. Yamazaki, Z. Siroma, H. Senoh, T. Ioroi, N. Fujiwara, and K. Yasuda, "A fuel cell with selective electrocatalysts using hydrogen peroxide as both an electron acceptor and a fuel," *Journal of Power Sources*, vol. 178, no. 1, pp. 20–25, 2008.
- [12] Y. Yang, Y. Xue, F. Huang, H. Zhang, K. Tao, R. Zhang, Q. Shen, and H. Chang, "A facile microfluidic hydrogen peroxide fuel cell with high performance: electrode interface and power-generation properties," *ACS Applied Energy Materials*, vol. 1, no. 10, pp. 5328–5335, 2018.
- [13] F. Yang, K. Cheng, T. Wu, Y. Zhang, J. Yin, G. Wang, and D. Cao, "Preparation of au nanodendrites supported on carbon fiber cloth and its catalytic performance to H₂O₂ electroreduction and electrooxidation," *RSC Advances*, vol. 3, no. 16, pp. 5483–5490, 2013.
- [14] X. Yan, A. Xu, L. Zeng, P. Gao, and T. Zhao, "A paper-based microfluidic fuel cell with hydrogen peroxide as fuel and oxidant," *Energy Technology*, vol. 6, no. 1, pp. 140–143, 2018.
- [15] L. An, T. Zhao, X. Yan, X. Zhou, and P. Tan, "The dual role of hydrogen peroxide in fuel cells," *Science Bulletin*, vol. 60, no. 1, pp. 55–64, 2015.
- [16] A. Sanli and A. Aytac, "Response to disselkamp: direct peroxide/peroxide fuel cell as a novel type fuel cell," *International Journal of Hydrogen Energy*, vol. 36, no. 1, pp. 869–875, 2011.
- [17] S. Hasegawa, K. Shimotani, K. Kishi, and H. Watanabe, "Electricity generation from decomposition of hydrogen peroxide," *Electrochemical and Solid-State Letters*, vol. 8, no. 2, p. A119, 2004.
- [18] A. A. Solovev, Y. Mei, E. Bermudez Urena, G. Huang, and O. G. Schmidt, "Catalytic microtubular jet engines self-propelled by accumulated gas bubbles," *Small*, vol. 5, no. 14, pp. 1688–1692, 2009.
- [19] A. A. Solovev, E. J. Smith, C. C. Bof Bufon, S. Sanchez, and O. G. Schmidt, "Light-controlled propulsion of catalytic microengines," *Angewandte Chemie International Edition*, vol. 50, no. 46, pp. 10 875–10 878, 2011.
- [20] S. Sanchez, A. A. Solovev, S. Schulze, and O. G. Schmidt, "Controlled manipulation of multiple cells using catalytic microbots," *Chemical Communications*, vol. 47, no. 2, pp. 698–700, 2011.
- [21] J. Simmchen, V. Magdanz, S. Sanchez, S. Chokmaviroj, D. Ruiz-Molina, A. Baeza, and O. G. Schmidt, "Effect of surfactants on the performance of tubular and spherical micromotors—a comparative study," *RSC Advances*, vol. 4, no. 39, pp. 20 334–20 340, 2014.
- [22] H. Wang, G. Zhao, and M. Pumera, "Crucial role of surfactants in bubble-propelled microengines," *The Journal of Physical Chemistry C*, vol. 118, no. 10, pp. 5268–5274, 2014.
- [23] W. Wang, W. Duan, A. Sen, and T. E. Mallouk, "Catalytically powered dynamic assembly of rod-shaped nanomotors and passive tracer particles," *Proceedings of the National Academy of Sciences*, vol. 110, no. 44, pp. 17 744–17 749, 2013.
- [24] Y. Ke and G. Fen, G. Yinyi, Z. Dongming, C. Kui, Z. Wenping, W. Guiling, and Cao, Dianxue. "Three-dimensional carbon-and binder-free nickel nanowire arrays as a high-performance and low-cost anode for direct hydrogen peroxide fuel cell," *Journal of Power Sources*, vol. 300, pp. 147–156, 2015.
- [25] N. Sac-Epee, MR. Palacin, A. Delahaye-Vidal, Y. Chabre, and J-M. Tara., "Evidence for Direct γ - NiOOH \leftrightarrow β - Ni (OH)₂ Transitions during Electrochemical Cycling of the Nickel Hydroxide Electrode," *J. of the Electrochemical Society*, vol. 545, no. 5, pp. 1434, 1998.